Appl. Math. & Math. Physics (Journal)

Прикладная математика и математическая физика
2015, том 1, №1, 77–100

DOI 10.18262/ammp.2015.0101-06

Elasticity Theory of Thin Plates and Active Optics. Solutions for Generating Toroid Surfaces with Vase Forms

Gérard R. Lemaitre

Abstract. The elasticity theory of thin plates is applied to appropriate mirror thickness distributions and external load configurations for generating optical aberration mode corrections. From the analysis and an experiment, it has been shown that the formulation of the net shearing force of this theory, as found in the classical literature, must be corrected as presented in this paper. The new formulation was validated and applied to meniscus form and vase form mirrors generating the correction of third-order astigmatism. Geometrical designs based on vase form thickness distributions also allow obtaining diffraction-limited deformations with a reduced set of four perimeter forces only. These active optics configurations, which show two concentric zones of constant thickness, are useful solutions to generate astigmatism corrections by a saddle-like flexure on flat or spherical surfaces – with glass or metal substrates – providing hyperbolic-paraboloid or toroid shapes respectively.

Keywords: elasticity theory, active optics, toroid surfaces, aspheric mirrors, optical aberrations.

MSC2010: 74-02, 74A99, 74B05, 78A05, 85-02

1. Introduction: elasticity and optics

Elasticity analyses and optical designs of mirrors for astronomy allow the optimization of substrate geometry with appropriate boundary conditions for obtaining an optical surface either by *stress polishing* or by *in-situ stressing*. For materials having a linear stress-strain relationship, such as glass and some metal alloys, these methods provide accurate optical deformation modes which fully satisfy *diffraction-limited criteria*. The highly accurate and remarkably *smooth surfaces* obtained from *active optics* methods allow to built new optical systems that use highly aspheric and non-axisymmetric (sometime called *freeform*) surfaces. The elasticity theory of thin plates is extremely useful for the research and optimization of obtaining aspheric surfaces with constant thickness distribution (CTD), this is mainly because CTD is the only way for superposing many optical modes.

The text submitted by the author in English.

Optimal elasticity configurations can be found by particular flexure of optical modes such as the curvature mode Cv1, represented in cylindrical coordinates by $z = A_{20}r^2$, or the three 3rd-order aberration modes: spherical aberration, coma and astigmatism – Sphe 3, Coma 3, Astm 3 – represented by $z \propto r^4$, $r^3\cos\theta$, $r^2\cos(2\theta)$, respectively, or some optical mode of the general form

$$z_{n,m} = A_{nm}r^n\cos(m\theta), \tag{1}$$

where n and m are integers such that $m \leqslant n$, $n+m$ is even, and $n+m \geqslant 2$. For $n+m \geqslant 4$, the *aberration order* of an optical mode is usually defined by the value $n+m-1$. The two first-order modes Tilt 1 and Cv 1 form the Gaussian terms of optics, or the dioptrics modes. The set of all $z_{n,m}$ optical modes belongs to a triangle matrix called the *Seidel modes*.

Applying a non-uniform load over all the surface of a plate is difficult, so for practical reasons we restrict here to cases of *circular plates* where only an external uniform load ($q = \text{const}$), or nothing ($q = 0$) are applied all over the clear optical aperture of a circular mirror. Generating by flexure a non-axisymmetric mode leads to applying force distributions along the mirror contour – modulated in $m\theta$ azimuthal angle – in order to provide the requested shearing forces and bending moments at the contour boundaries. Axisymmetric and non-axisymmetric flexural modes of a circular plate where first derived by Poisson and Clebsch respectively. These results are reduced to solve the bi-laplacian equation $\nabla^2\nabla^2 z - q/D = 0$, where D is a constant (called rigidity) related to the plate thickness t by $D \propto t^3$. The flexural modes which are solutions of this equation are called *Clebsch modes*.

Investigations carried out with variable thickness distribution (VTD) circular plates [1] for obtaining Seidel modes generally lead to configurations which do not allow the superposition of the modes, or coadding modes, except for Cv 1 and Astm 1 which both have the same cycloid-like VTD. In order to achieve a high degree of aberration correction, the main goal of optics is to fully benefit from the coaddition capability of elastic modes, then to obtain aspheric optical mirrors which could provide the best imaging quality. Compared to VTDs, the reason of coaddition capability leads us to investigate hereafter only the case of constant thickness distributions (CTD).

Research of configurations where the flexural Clebsch modes have the same form as optical Seidel modes is investigated for two configuration classes: *single thickness* plates and *double concentric zone* plates, with one or two constant zonal thicknesses, i.e., mirror plates belonging to CTDs. For mirrors having a moderate optical power, these configurations are called *meniscus forms* and *vase forms* respectively.

2. Elasticity theory of thin plates with constant thickness distributions (CTDs)

Because of differences in the homogeneity of sign conventions found in books and literature on thin plate deformations, it seems useful to reformulate hereafter the classic theory of thin plates.

For further simplification in the notations, let's denote the *rigidity* D of a plate as related to its thickness t by

$$D = \frac{Et^3}{12(1-\nu^2)}, \tag{2}$$

where the Young's modulus E and Poisson's ratio ν are constants depending on the material.

In the case of plates with a variable thickness distribution (VTD) the rigidity D is not a constant. Theoretical investigations of axisymmetric thickness plates – i.e., rigidity of the form $D(r)$ – lead to obtain flexural modes satisfying the Seidel modes with very simple boundary conditions [1], [2]. Nevertheless, due to the extreme difficulty to realize the superposition of these flexural mode, we restrict to the case of constant thickness distributions (CTD), i.e., D is a constant.

Considering CTD plates and a cylindrical coordinate system, the radial and tangential bending moments and the twisting moment, per unit length, can be defined by

$$M_r = D\left[\frac{\partial^2 z}{\partial r^2} + \nu\left(\frac{1}{r}\frac{\partial z}{\partial r} + \frac{1}{r^2}\frac{\partial^2 z}{\partial \theta^2}\right)\right], \tag{3$_1$}$$

$$M_t = D\left[\frac{1}{r}\frac{\partial z}{\partial r} + \frac{1}{r^2}\frac{\partial^2 z}{\partial \theta^2} + \nu\frac{\partial^2 z}{\partial r^2}\right], \tag{3$_2$}$$

$$M_{rt} = M_{tr} = (1-\nu)D\left[\frac{1}{r^2}\frac{\partial z}{\partial \theta} - \frac{1}{r}\frac{\partial^2 z}{\partial r\,\partial \theta}\right], \tag{3$_3$}$$

where *a positive flexure entails a positive radial bending moment M_r applied at $r = a$ for generating the fundamental* Cv 1 *mode $z_{20} = A_{20}r^2$ (curvature mode)*. For z_{nm} modes with $m = n$, we may also verify that M_r is positive in the x, z section, $y = \theta = 0$. This sign convention is natural and in agreement with the generally used optics convention *a curved surface z_{20} is of positive curvature if* $\forall\, r$, $z_{20}(r) > z_{20}(0)$.

Since the Laplacian is

$$\nabla^2 z = \frac{\partial^2 z}{\partial r^2} + \frac{1}{r}\frac{\partial z}{\partial r} + \frac{1}{r^2}\frac{\partial^2 z}{\partial \theta^2}, \tag{4}$$

the bending moments satisfy

$$M_r + M_t = (1+\nu)D(r,\theta)\nabla^2 z. \tag{5}$$

The determination of radial and tangential shearing forces, Q_r and Q_t respectively, as functions of the flexural moments, is derived from the equilibrium of a segment element $r\,d\theta\,dr$ around the tangential axis $O\tau'$ parallel to $\omega\tau$ and around the radial axis $O\omega$ respectively (Fig. 1).

For the radial shearing force Q_r the resulting components around $O\tau'$ are

$$Q_r\, r\, d\theta\, dr + \frac{\partial}{\partial r}(rM_r)\, d\theta\, dr - M_t\, d\theta\, dr - \frac{\partial M_{rt}}{\partial \theta}\, d\theta\, dr = 0,$$

where the third term is the sum of two components tilted of $\pm\, d\theta/2$ from the radial axis $O\omega$. After simplification and use of equations (3), the radial shearing force is represented by

$$Q_r = -\frac{\partial M_r}{\partial r} - \frac{1}{r}\left(M_r - M_t - \frac{\partial M_{rt}}{\partial \theta}\right) = -D\,\frac{\partial}{\partial r}\,(\nabla^2 z). \tag{6}$$

The tangential shearing force Q_t is derived from the moments around $O\omega$. The resulting components are

$$Q_t\, r\, d\theta\, dr + \frac{\partial M_t}{\partial \theta}\, d\theta\, dr - M_{rt}\, d\theta\, dr - \frac{\partial}{\partial r}(rM_{rt})\, d\theta\, dr = 0,$$

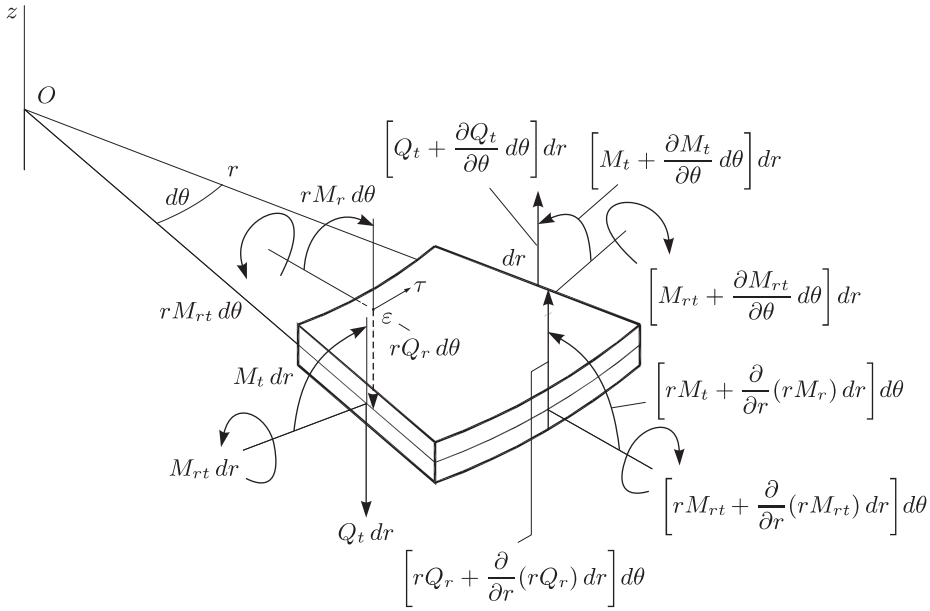

Fig. 1. Bending moments, twisting moment and shearing force providing the equilibrium of plate element $r\,d\theta\,dr$

and after simplification and use of equations (3) the tangential shearing force is

$$Q_t = -\frac{1}{r}\left(\frac{\partial M_t}{\partial \theta} - 2\,M_{rt}\right) + \frac{\partial M_{rt}}{\partial r} = -D\,\frac{1}{r}\frac{\partial}{\partial \theta}\,(\nabla^2 z). \tag{7}$$

The net shearing force V_r, first derived by Kirchhoff [3], [4], takes into account the variation of the twisting moment M_{rt}. Accordingly to the sign convention for the three flexural moments, the net shearing force [5] is [1]

$$V_r = Q_r - \frac{1}{r}\,\frac{\partial M_{rt}}{\partial \theta}. \tag{8}$$

The force V_r, which represents the axial resultant acting at a plate radius r, is useful to define a boundary condition (known as *Kirchhoff's condition*) at the edge:

[1] The present positive sign convention for the bending moments M_r and M_t – cf. in detail below equations (3) – provides a logical representation of the flexure. It was used independently by Lubliner and Nelson [6] without comments. However, a negative sign convention has been used by other authors. As shown here in Fig. 1, the variation of the bending moment M_r along the radial direction entails that a positive curvature mode z_{20} is generated by a positive bending moment M_r for increasing values of radius r.

There is an error in *Theory of Plates and Shells* by Timoshenko and Woinowsky-Krieger [7, at Eq. (j), p. 284]: their convention uses a negative sign in the definition of the three moments M_r, M_t and M_{rt}, while the sign of their shearing forces Q_r and Q_t with respect to the Laplacian term is as in above equations (6) and (7). Hence the correctly associated representation of the net shearing force should be $V_r = Q_r + \partial M_{rt}/(r\,\partial r)$, with their notation.

Several other authors use negative sign convention from [7] or the present positive sign convention in defining the two bending moments, but the torsion moment M_{rt} appears with an opposite sign whatever convention used. In order to respect the equilibrium equations of statics, the sign before M_{rt} is also changed in those equations, so the Poisson biharmonic equation is satisfied. However, there is an error in the sign before $\partial M_{rt}/(r\,\partial r)$. A similar error in the definition of V_r seems also to appear in the article by E. Reissner [8].

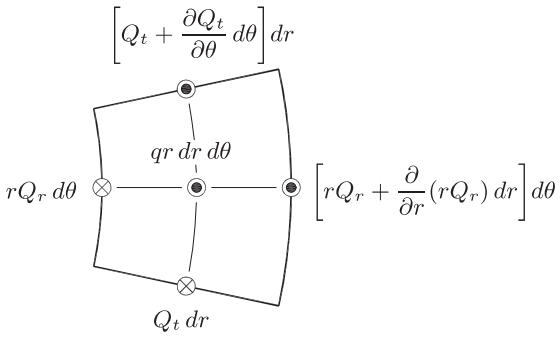

Fig. 2. External uniform load q applied to a plate element and shearing forces providing the equilibrium of a plate element in z-direction

if a plate has a *free edge*, then $V_r = 0$ at its contour. Since D is a constant, after substitution of Q_r and M_{rt}, we obtain

$$V_r = -D\,\frac{\partial}{\partial r}\,(\nabla^2 z) + (1-\nu)\,D\,\frac{1}{r}\,\frac{\partial}{\partial r}\left(\frac{1}{r}\,\frac{\partial^2 z}{\partial \theta^2}\right). \tag{9}$$

The external uniform load q, applied per unit area onto the surface of the elementary segment, is in static equilibrium with the shearing forces (Fig. 2). After dividing the terms of the equilibrium equation by element area $r\,d\theta\,dr$ we have

$$\frac{1}{r}\,\left[\frac{\partial}{\partial r}(rQ_r) + \frac{\partial Q_t}{\partial \theta}\right] + q = 0. \tag{10}$$

This partial derivative equation linking the shearing forces to a uniform load q is a general relation applying either to variable thickness plates (VTD) or constant thickness plates (CTD). Restricting to the case of constant thickness plates for reasons of coaddition mode capability (see Section 1), i.e., D is a constant, we obtain from equations (6) and (7)

$$\nabla^2\nabla^2 z(r,\theta) - \frac{q}{D} = 0, \qquad D = \frac{Et^3}{12(1-\nu^2)} = \text{const}, \tag{11}$$

which is the fundamental biharmonic equation of thin plate theory of circular plate [7], [8], also called *Poisson's equation* of elasticity.

Case 1. Null uniform load: $q = 0$. The general solutions of equation (11) are of the form

$$Z = R_{n0} + \sum_{m=1}^{\infty} R_{nm}\cos(m\theta) + \sum_{m=1}^{\infty} R'_{nm}\sin(m\theta), \tag{12}$$

where $R_{n0}, R_{n1}, \ldots, R'_{n1}, \ldots$ are function of the radial distance only. For simplification, we restrict this study to deformation terms with cosine azimuth only, as proposed by equation (1), for obtaining optical modes $z_{n,m}$ (also denoted z_{nm}). Then we consider hereafter only terms where R'_{nm} vanish:

$$R'_{nm}(r) = 0.$$

Quantities $R_{nm}(r)$ are solutions of

$$\left(\frac{d^2}{dr^2}+\frac{1}{r}\frac{d}{dr}-\frac{m^2}{r^2}\right)\left(\frac{d^2R_{nm}}{dr^2}+\frac{1}{r}\frac{dR_{nm}}{dr}-\frac{m^2}{r^2}R_{nm}\right)=0. \tag{13}$$

For $m=0, m=1$ and $m>1$, the functions R_{nm} of the general solutions (called *Clebsch's polynomials* [10]) have the following forms:

$$R_{n0}=B_{n0}+C_{n0}\ln r+D_{n0}r^2+E_{n0}r^2\ln r, \tag{14_1}$$
$$R_{n1}=B_{n1}r+C_{n1}r^{-1}+D_{n1}r^3+E_{n1}r\ln r, \tag{14_2}$$
$$R_{nm}=B_{nm}r^m+C_{nm}r^{-m}+D_{nm}r^{m+2}+E_{nm}r^{-m+2}. \tag{14_3}$$

Case 2. Uniform load: $q=$ const. The general solution of the biharmonic equation (11) is unique and axisymmetric, i.e., $R_{nm}=0$ for $m\neq 0$. It is then parented to equation (14_1) but includes a fifth term in r^4:

$$R_{n0}=\frac{q}{64D}\,r^4+B_{n0}+C_{n0}\ln r+D_{n0}r^2+E_{n0}r^2\ln r. \tag{14_4}$$

NB The logarithm terms in equations (14_1) and (14_4), $C_{n0}\ln r$ and $E_{n0}r^2\ln r$, apply to *holed plates*, whilst the $E_{n0}r^2\ln r$ term alone relates to a *concentrated load acting at the center* of the circular plate.

3. Solution families generating seidel optical modes

One usually characterizes the optical power of a mirror of curvature $1/R$ and clear aperture d by its *aperture-ratio* $f/d=R/(2d)$. For mirrors with relatively low f-ratios, say, $f/5$ (i.e., $f/d=5$), $f/4$, up to $f/3$, the sag due to its curvature is relatively low, so the stresses induced in the middle surface of the meniscus plate remain very low and do not require using the theory of shallow spherical shells [1]. Assuming that this condition is fulfilled, the thin plate theory is applied to either CTD plane mirrors or CTD meniscus mirrors.

We research configurations able to generate flexure of a CTD circular plate identical to the shape of a wavefront optical mode, also called *Seidel mode*. These modes belong to a circular polynomial series. Each mode is represented by

$$z\equiv z_{nm}=A_{nm}r^n\cos(m\theta),\qquad m\leqslant n,\quad m+n\geqslant 2, \tag{15}$$

where $m+n$ is even, n and m are integers. Given the condition $m\leqslant n$, the series development of such optics modes generates the terms of a *triangular matrix*. For low-order modes we use the simple suffix denotation nm instead of n,m. With $m+n=4$, the three terms coming after the dioptrics are the primary aberration modes z_{40}, z_{31} and z_{22}, i.e., spherical aberration, coma and astigmatism respectively, also denoted Sphe 3, Coma 3 and Astm 3.

The following derivative elements:

$$\frac{\partial^2 z}{\partial r^2} = n(n-1)A_{nm}r^{n-2}\cos(m\theta), \tag{16$_1$}$$

$$\frac{1}{r}\frac{\partial z}{\partial r} + \frac{1}{r^2}\frac{\partial^2 z}{\partial \theta^2} = (n-m^2)A_{nm}r^{n-2}\cos(m\theta), \tag{16$_2$}$$

$$\nabla^2 z = [n(n-1)+(n-m^2)]A_{nm}r^{n-2}\cos(m\theta), \tag{16$_3$}$$

allow determining of the bilaplacian $\nabla^2\nabla^2 z$. After substitution in (11), we obtain

$$A_{nm}\,(n^2-m^2)[(n-2)^2-m^2]r^{n-4}\cos(m\theta) - \frac{q}{D} = 0, \qquad n \geqslant 2. \tag{17}$$

The Clebsch solutions – combinations of n and m for which the equation can be solved for practicable applications (i.e., uniform load $q = 0$ or $q = \text{const}$) – are

$$\begin{aligned}
&\text{Case 1:} \quad q = 0 \quad &&\longrightarrow \quad m = n, \quad &&\text{i.e., } z_{22}, z_{33}, z_{44}, \ldots \text{ terms,} \\
&\qquad\qquad\quad\;\; &&\longrightarrow \quad m = n-2, \quad &&\text{i.e., } z_{20}, z_{31}, z_{42}, \ldots \text{ terms,} \\
&\text{Case 2:} \quad q = \text{const} &&\longrightarrow \quad n = 4,\ m = 0, \quad &&\text{i.e., the } z_{40} \text{ term.}
\end{aligned} \tag{18}$$

These solutions belong to a *subclass* of Seidel modes to be called *Clebsch–Seidel modes*.

Except for z_{40} mode, the other modes belong to the two lower diagonals of the optics triangular matrix (Fig. 3). The generation of $z_{20} \equiv \text{Cv}\,1$, $z_{40} \equiv \text{Sphe}\,3$,

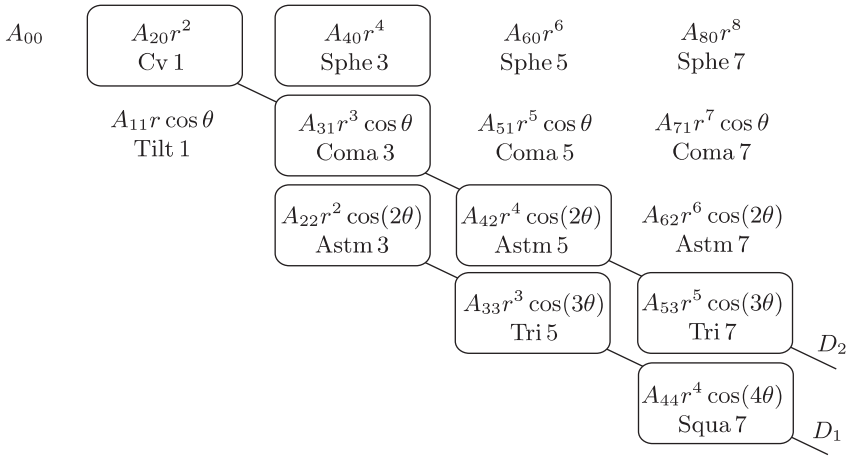

Fig. 3. Triangular matrix of optical Seidel modes. Except for spherical aberration mode Sphe 3, the subclass of Clebsch–Seidel modes (shown in boxes) is represented by the diagonal lines $m = n$ and $m = n-2$

$z_{31} \equiv \text{Coma}\,3$, $z_{22} \equiv \text{Astm}\,3$, $z_{42} \equiv \text{Astm}\,5$, $z_{33} \equiv \text{Tri}\,5$, $z_{53} \equiv \text{Tri}\,7$, $z_{44} \equiv \text{Squa}\,7$, ... modes is obtained, while it is found not possible to generate the two other 5^{th}-order modes $z_{51} \equiv \text{Coma}\,5$ or $z_{60} \equiv \text{Sphe}\,5$ by only using $q = 0$ or $q = \text{const}$. Generating z_{51} would require a prismatic loading; generating z_{60}, a parabolic loading. Due to extreme difficulties to achieve them in practice, such non-uniform loading distributions are not considered hereafter.

4. Meniscus form mirrors generating Clebsch–Seidel modes

The bending and twisting moments, as derived from equations (3), are

$$M_r = D[n(n-1) + \nu(n-m^2)]A_{nm} r^{n-2}\cos(m\theta), \tag{19$_1$}$$

$$M_t = D[n - m^2 + \nu n(n-1)]A_{nm} r^{n-2}\cos(m\theta), \tag{19$_2$}$$

$$M_{rt} = D[m(n-1)(1-\nu)]A_{nm} r^{n-2}\sin(m\theta). \tag{19$_3$}$$

By (6) and (9), the radial shearing force Q_r and the net shearing force V_r are

$$Q_r = -D[(n-2)(n^2-m^2)]A_{nm} r^{n-3}\cos(m\theta), \tag{20}$$

$$V_r = -D[(n-2)(n^2-m^2) + (1-\nu)(n-1)m^2]A_{nm} r^{n-3}\cos(m\theta). \tag{21}$$

For each of the first flexural modes, the bending moment M_r and shearing forces Q_r and V_r at the mirror perimeter $r = a$ and at $\theta = 0$ are following:

Mode	n	m	$M_r(a,0)$	$Q_r(a,0)$	$V_r(a,0)$	
Cv 1	2	0	$2(1+\nu)DA_{20}$	0	0	(22$_1$)
Sphe 3*	4	0	$4(3+\nu)Da^2A_{40}$	$-32DaA_{40}$	$-32DaA_{40}$	(22$_2$)
Coma 3	3	1	$2(3+\nu)DaA_{31}$	$-8DA_{31}$	$-2(5-\nu)DA_{31}$	(22$_3$)
Astm 3	2	2	$2(1-\nu)DA_{22}$	0	$-4(1-\nu)Da^{-1}A_{22}$	(22$_4$)
Astm 5	4	2	$12Da^2A_{42}$	$-24DaA_{42}$	$-12(3-\nu)DaA_{42}$	(22$_5$)
Tri 5	3	3	$6(1-\nu)DaA_{33}$	0	$-18(1-\nu)DA_{33}$	(22$_6$)

* for Sphe 3 mode, the uniform loading is $q = 64DA_{40}$.

For generating a non-axisymmetric mode, the required boundary conditions at the contour $r = a$ are defined from the associated bending moment $M_r(a,\theta)$ and net shearing force $V_r(a,\theta)$. This requires use of K radial arms *clamped* to the mirror contour (Fig. 4).

The total number K of implemented radial arms depends on the type of mode and on the number of modes to be superposed. The rigidity of the meniscus must be optimized for an admissible stress level of the material. The intensity of axial forces $F_{a,k}$ and $F_{c,k}$ to apply, at $r = a$ and $r = c$ (at the end of radial arms clamped onto the edge), are derived from static equilibrium relationships

$$F_{a,k} + F_{c,k} = a\int_{\pi(2k-3)/K}^{\pi(2k-1)/K} V_r(a,\theta)\,d\theta, \tag{23$_1$}$$

$$(c-a)F_{c,k} = a\int_{\pi(2k-3)/K}^{\pi(2k-1)/K} M_r(a,\theta)\,d\theta, \tag{23$_2$}$$

$k = 1, 2, \ldots, K$ for a mirror having K radial arms.

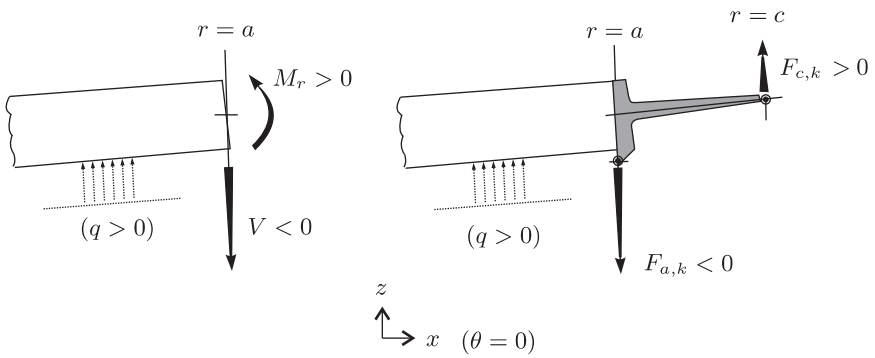

Fig. 4. Sign convention: meniscus form deformable mirror. By K we clamped arms are angularly and uniformly distributed around the mirror. Axial forces $F_{a,k}$ and $F_{c,k}$ act respectively at radii $r = a$ and $r = c$ at the ends of radial arm number k. These forces are derived from M_r and V_r. For the single curvature mode $z = A_{20}r^2$, if A_{20} is positive, then the curvature is positive and the sign convention gives also $M_r > 0$

Coaddition of various modes is obtained by summing the corresponding forces. The resulting forces to apply, $\mathcal{F}_{a,k}$ and $\mathcal{F}_{c,k}$, are

$$\mathcal{F}_{a,k} = \sum_{n,m \text{ modes}} F_{a,k}, \qquad \mathcal{F}_{c,k} = \sum_{n,m \text{ modes}} F_{c,k}. \tag{24}$$

The resulting mirror geometry with radial arms built-in along the contour and allowing coaddition of various modes is called hereafter a *multimode deformable mirror*, or MDM.

5. Meniscus form with special arm geometry for the astigmatism mode

The 3rd-order astigmatism aberration, Astm 3, is an off-axis aberration which appears on any optical beams reflected by a convex or concave spherical mirror when the principal ray of the beam is not reflected perpendicularly to the mirror surface, i.e., when this beam is deviated by the mirror.

Generating the Astm 3 mode by active optics on a meniscus mirror requires use of a minimum number of four radial arms, $K = 4$, angularly distributed at $\theta = 0, \pi/2, \pi$ and $3\pi/2$. This would generally entail applying a set of four forces $F_{a,k}$ at the mirror edge $r = a$ and a set of four forces $F_{c,k}$ at the outer ends of the arms $r = c$. However, a special design with only four $F_{c,k}$ forces can be obtained by ensuring the convenient distributions of $M_r(a, \theta)$ and $V_r(a, \theta)$. Stating that $F_{a,k} = 0$, we obtain from $k = 1$ to $k = 4$, by equations (23),

$$\int_{\pi(2k-3)/4}^{\pi(2k-1)/4} V_r(a, \theta)\, d\theta = \frac{1}{a - c} \int_{\pi(2k-3)/4}^{\pi(2k-1)/4} M_r(a, \theta)\, d\theta. \tag{25}$$

After substitution of M_r and V_r by their values in (22_4) the radial value c of the arm end is

$$c = \frac{a}{2}. \tag{26}$$

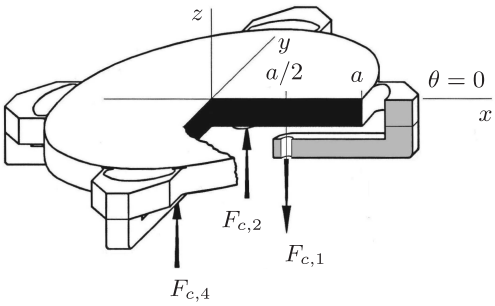

Fig. 5. Configuration of a four-arm meniscus-form mirror generating Astm 3 mode. It uses only two pairs of opposite forces $F_{c,1}{=}{-}F_{c,2}{=}F_{c,3}{=}{-}F_{c,4}$ acting at radius $c = a/2$ on folded arm ends located in directions x and y. Since $\forall F_{a,k}{=}0$, we avoid using eight forces and call it a degenerated configuration. The boundaries are realized via arches linked to the mirror edge by two thin tangential stripes, separated by 22.5°, providing a best azimuth modulation in $\cos(2\theta)$ for generating M_r and V_r

This very simple geometry reducing the number of forces from eight to four is called *degenerated configuration*. The four arms must be folded towards the mirror center (Fig. 5): *a meniscus form of clear aperture* $2a$ *provides a pure* 3^{rd}*-order astigmatic flexure* Astm 3 *by requiring only four alternatively opposite forces* $F_{c,k}$ *applied to the ends of folded arms at radial distance* $c = a/2$.

The set of four forces $F_{c,k}$ is by itself in equilibrium – or self-reacting. The force intensities and directions are, by (23_1),

$$F_{c,k} = (-1)^k 4(1-\nu)DA_{22} = (-1)^k \frac{Et^3}{3(1+\nu)} A_{22}, \qquad k = 1, 2, 3, 4. \tag{27}$$

NB One can show as a general result that Clebsch–Seidel modes with $m = n$, such as Tri 5 mode $A_{33}r^3\cos(3\theta)$, can benefit from these simple degenerated configurations where $F_{a,k} = 0$ [1].

6. Vase form and multimode deformable mirrors (MDMs)

6.1. Saint-Venant's principle of equivalence and vase form

In order to generate very smooth optical surfaces by active optics, one has to avoid or minimize the effects of local deformations at the regions where the forces are applied. These local deformations are well known from analyses using the thick plate theory [7] which takes into account the shear stresses and shows that the amplitude of the flexure varies along the thickness of the plate and is a maximum where the forces are applied.

With the meniscus plate used in the previous section for correcting astigmatism, the proximity of the forces applied at the mirror contour entails to build a mirror somewhat larger than that of its clear aperture. Another alternative to avoid these local deformations at the mirror surface is to develop a *vase form* design. It is made of two concentric zones, each of them of constant thickness, with the outer ring thicker than the inner meniscus. The diameter of the meniscus corresponds to that of the clear mirror aperture.

Saint-Venant enounced a useful principle which introduced some flexibility for practical applications of the boundary conditions [2]. We recall that a set of forces define a torsor which, at any given point, is globally represented by a resultant force and a resultant moment. An excellent statement of Saint-Venant's principle of equivalence has been given by Germain and Muller [12] as follows: *if one substitutes a first distribution of given surface forces* $\mathbf{F}$, *acting on a part* $\delta\mathcal{A}_B$ *of a boundary area, by a second one acting on the neighborhood and determining the same torsor, whilst the other boundary conditions on the complementary parts of* $\mathcal{A}_B$ *relatively to* $\mathcal{A}$ *remain unchanged, then in all regions of* $\mathcal{A}$ *sufficiently distant from* $\mathcal{A}_B$ *the stress and strain components are practically unchanged.*

The application of Saint-Venant's principle allows determining *equivalent loading configurations* at the contour of a solid (Fig. 6).

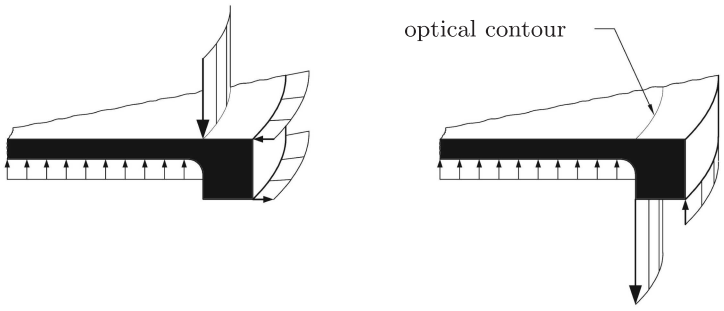

Fig. 6. Saint-Venant's principle of equivalence: example of two equivalent load configurations applied at the boundary of an axisymmetric vase form mirror. The optical clear aperture is that of the junction zone. Configuration on right: local deformations at force application zones will not affect the optical figure

6.2. Vase form and radial arms geometrical design

Let us consider a plane MDM with a clear aperture zone defined by $0 \leqslant r < a$, a built-in ring zone defined by $a < r \leqslant b$, where t_1, t_2 and D_1, D_2 are the thicknesses and associated rigidities of the inner and outer zones, respectively. The axial forces applied to the ring inner radius, $r = a$, are denoted by $F_{a,k}$; those applied to the arm outer-end, at $r = c$, by $F_{c,k}$. With a total number of K arms, each arm is numbered by $k \in [1, 2, \ldots, K]$ and $k = 1 \Leftrightarrow \theta = 0$. In addition, positive or negative uniform loads q can be superposed into the vase inner zone by mean of air pressure or depressure (Fig. 7).

• *Inner and outer zone – Rigidity ratio.* The constant rigidities of inner and outer zones of the vase form can be denoted by D_1 and D_2, respectively, where

$$\begin{aligned} D_1 &= \frac{Et_1^3}{12(1-\nu^2)}, \qquad 0 \leqslant r \leqslant a, \\ D_2 &= \frac{Et_2^3}{12(1-\nu^2)}, \qquad a \leqslant r \leqslant b. \end{aligned} \tag{28}$$

[2] Saint-Venant first enounced the equivalence principle in *Sur la Torsion des Prismes* [11, p. 298–299].

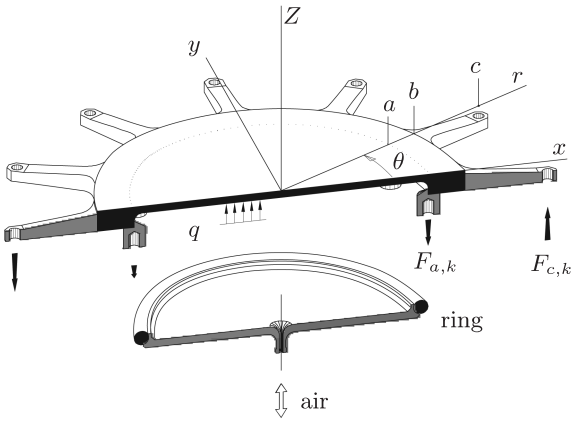

Fig. 7. Elasticity design of a vase form MDM based on two concentric rigidities and radial arms. The clear aperture zone is built-in at $r = a$ into a thicker ring. This holosteric design allows generating and coadding the Clebsch–Seidel deformation modes, Cv 1, Sphe 3, Coma 3, Astm 3, etc., by axial forces $F_{a,k}$ and $F_{c,k}$ applied at the ring inner radius $r = a$ and outer end $r = c$ of K arms

Let us introduce the *rigidity ratio* γ between the two zones as

$$\gamma = \frac{D_1}{D_2} = \frac{t_1^3}{t_2^3}, \tag{29}$$

where $\gamma < 1$ for a vase form.

• *Continuity conditions.* The continuity conditions on z, $\partial z/\partial r$, M_r and V_r at the junction $r = a$, $\forall\,\theta$ after simplifications are, respectively,

$$A_{nm} a^n = R_{nm}(a), \tag{30$_1$}$$

$$A_{nm} n a^{n-1} = \left[\frac{dR_{nm}}{dr}\right]_{r=a}, \tag{30$_2$}$$

$$A_{nm}\big[n(n-1) + \nu(n-m^2)\big]a^{n-2} = \frac{1}{\gamma}\left[\frac{d^2R_{nm}}{dr^2} + \frac{\nu}{r}\frac{dR_{nm}}{dr} - \frac{\nu m^2}{r^2}R_{nm}\right]_{r=a}, \tag{30$_3$}$$

$$A_{nm}\big[(n-2)(n^2-m^2) + (1-\nu)(n-1)m^2\big]a^{n-3} = \frac{1}{\gamma}\left[\frac{d^3R_{nm}}{dr^3} + \frac{1}{r}\frac{d^2R_{nm}}{dr^2} - \frac{1+\nu m^2}{r^2}\frac{dR_{nm}}{dr} + \frac{(1+\nu)m^2}{r^3}R_{nm}\right]_{r=a}. \tag{30$_4$}$$

The above set allows to determine the constants B_{nm}, C_{nm}, D_{nm} and E_{nm} in equations (14) as functions of A_{nm}, and then the bending moment $M_r(b,\theta)$ and net shearing force $V_r(b,\theta)$ distributions to apply at the ring outer edge $r = b$.

• *First Clebsch–Seidel modes.* For the first Clebsch–Seidel modes, the substitution of each z_{nm} mode into equations (30) and solving of the associate system set lead to the following relation sets:

Curvature 1st-order mode – Cv 1 ($n = 2$, $m = 0$):

$$\begin{aligned}
B_{20} &= (1-\gamma)(1+\nu)(1-\ln a^2)\frac{a^2 A_{20}}{2},\\
C_{20} &= (1-\gamma)(1+\nu)a^2 A_{20},\\
D_{20} &= [2-(1-\gamma)(1+\nu)]\frac{A_{20}}{2},\\
E_{20} &= 0,\\
M_r(b,0) &= D_2\Bigg[-(1-\nu)\frac{C_{20}}{b^2} + 2(1+\nu)D_{20}\\
&\qquad + (3+\nu)E_{20} + (1+\nu)E_{20}\ln b^2\Bigg],\\
Q_r(b,0) &= -4D_2\frac{E_{20}}{b},\\
V_r(b,0) &= Q_r(b,0).
\end{aligned} \tag{31$_1$}$$

Spherical aberration 3rd-order mode – Sphe 3 ($n = 4$, $m = 0$, $q = 64D_1A_{40}$):

$$\begin{aligned}
B_{40} &= \big\{\nu+\gamma(5-\nu)-[(1+\nu)+\gamma(1-\nu)]\ln a^2\big\}a^4 A_{40},\\
C_{40} &= 2[(1+\nu)+\gamma(1-\nu)]a^4 A_{40},\\
D_{40} &= [1-\nu-\gamma(5-\nu+4\ln a^2)]a^2 A_{40},\\
E_{40} &= 8\gamma a^2 A_{40},\\
M_r(b,0) &= D_2\Bigg[-(1-\nu)\frac{C_{40}}{b^2} + 2(1+\nu)D_{40}\\
&\qquad + (3+\nu)E_{40} + (1+\nu)E_{40}\ln b^2\Bigg],\\
Q_r(b,0) &= -4D_2\frac{E_{40}}{b},\\
V_r(b,0) &= Q_r(b,0).
\end{aligned} \tag{31$_2$}$$

Coma 3rd-order mode – Coma 3 ($n = 3, m = 1$):

$$\begin{aligned}
B_{31} &= (1-\gamma)[3+\nu-(1-\nu)\ln a^2]\frac{a^2 A_{31}}{2},\\
C_{31} &= -(1-\gamma)(1+\nu)\frac{a^4 A_{31}}{2},\\
D_{31} &= \gamma A_{31},\\
E_{31} &= (1-\gamma)(1-\nu)a^2 A_{31},\\
M_r(b,0) &= D_2\Bigg[2(1-\nu)\frac{C_{31}}{b^3} + 2(3+\nu)D_{31}b + (1+\nu)\frac{E_{31}}{b}\Bigg],\\
Q_r(b,0) &= -2D_2\Bigg[4D_{31} - \frac{E_{31}}{b^2}\Bigg],\\
V_r(b,0) &= -D_2\Bigg[-2(1-\nu)\frac{C_{31}}{b^4} + 2(5-\nu)D_{31} - (1+\nu)\frac{E_{31}}{b^2}\Bigg].
\end{aligned} \tag{31$_3$}$$

Astigmatism 3$^{\mathrm{rd}}$-order mode – Astm 3 ($n = 2$, $m = 2$):

$$
\begin{aligned}
B_{22} &= [4 + (1-\gamma)(1-\nu)]\frac{A_{22}}{4},\\
C_{22} &= -(1-\gamma)(1-\nu)\frac{a^4 A_{22}}{12},\\
D_{22} &= -(1-\gamma)(1-\nu)\frac{a^{-2} A_{22}}{6},\\
E_{22} &= 0,\\
M_r(b,0) &= 2D_2\left[(1-\nu)B_{22} + 3(1-\nu)\frac{C_{22}}{b^4} + 6D_{22}b^2 - 2\nu\frac{E_{22}}{b^2}\right],\\
Q_r(b,0) &= -8D_2\left[3D_{22}b + \frac{E_{22}}{b^3}\right],\\
V_r(b,0) &= -4D_2\left[(1-\nu)\frac{B_{22}}{b} - 3(1-\nu)\frac{C_{22}}{b^5}\right.\\
&\qquad \left. + 3(3-\nu)D_{22}b + (1+\nu)\frac{E_{22}}{b^3}\right].
\end{aligned}
\tag{31$_4$}
$$

Astigmatism 5$^{\mathrm{th}}$-order mode – Astm 5 ($n = 4$, $m = 2$):

$$
\begin{aligned}
B_{42} &= 3(1-\gamma)(3-\nu)\frac{a^2 A_{42}}{4},\\
C_{42} &= -(1-\gamma)(1+\nu)\frac{a^6 A_{42}}{4},\\
D_{42} &= [\gamma - (1-\gamma)(1-\nu)]\frac{A_{42}}{4},\\
E_{42} &= -3(1-\gamma)(1-\nu)\frac{a^4 A_{42}}{4},\\
M_r(b,0) &= 2D_2\left[(1-\nu)B_{42} + 3(1-\nu)\frac{C_{42}}{b^4} + 6D_{42}b^2 - 2\nu\frac{E_{42}}{b^2}\right],\\
Q_r(b,0) &= -8D_2\left[3D_{42}b + \frac{E_{42}}{b^3}\right],\\
V_r(b,0) &= -4D_2\left[(1-\nu)\frac{B_{42}}{b} - 3(1-\nu)\frac{C_{42}}{b^5}\right.\\
&\qquad \left. + 3(3-\nu)D_{42}b + (1+\nu)\frac{E_{42}}{b^3}\right].
\end{aligned}
\tag{31$_5$}
$$

Triangle 5$^{\mathrm{th}}$-order mode – Tri 5 ($n = 3$, $m = 3$):

$$
\begin{aligned}
B_{33} &= [2 + (1-\gamma)(1-\nu)]\frac{A_{33}}{2},\\
C_{33} &= -(1-\gamma)(1-\nu)\frac{a^6 A_{33}}{8},\\
D_{33} &= -3(1-\gamma)(1-\nu)\frac{a^{-2} A_{33}}{8},\\
E_{33} &= 0,
\end{aligned}
$$

$$M_r(b,0) = 2D_2\Bigg[3(1-\nu)B_{33}b + 6(1-\nu)\frac{C_{33}}{b^5} + 2(5-\nu)D_{33}b^3 + (1-5\nu)\frac{E_{33}}{b^3}\Bigg],$$

$$Q_r(b,0) = -24D_2\left[2D_{33}b^2 + \frac{E_{33}}{b^4}\right], \tag{31$_6$}$$

$$V_r(b,0) = -6D_2\Bigg[3(1-\nu)B_{33} - 6(1-\nu)\frac{C_{33}}{b^6} + 2(7-3\nu)D_{33}b^2 + (1+3\nu)\frac{E_{33}}{b^4}\Bigg].$$

• *Monomode forces $F_{a,k}$ and $F_{c,k}$.* In order to generate the bending moments M_r and net shearing forces V_r at $r = b$ for a given mode z_{nm}, we remark that the MDM design gains in *compactness* by applying axial forces at $r = a$ and $r = c$, not at $r = b$ and $r = c$. For each mode (n, m), the corresponding axial forces, denoted by $F_{a,k}$ and $F_{c,k}$, are determined from the statics equilibrium equations (see Fig. 7):

$$F_{a,k} + F_{c,k} = b\int_{\pi(2k-3)/K}^{\pi(2k-1)/K} V_r(b,\theta)\,d\theta, \tag{32$_1$}$$

$$(a-b)F_{a,k} + (c-b)F_{c,k} = b\int_{\pi(2k-3)/K}^{\pi(2k-1)/K} M_r(b,\theta)\,d\theta, \tag{32$_2$}$$

$k = 1, 2, \ldots, K$ for a MDM having K arms.

• *Resultant multimode forces $\mathcal{F}_{a,k}$ and $\mathcal{F}_{c,k}$.* The forces $F_{a,k}$ and $F_{c,k}$ are determined for each mode by solving the system (32). The coaddition of various modes is obtained by summing the corresponding forces. The resultant forces $\mathcal{F}_{a,k}$ and $\mathcal{F}_{c,k}$ to apply to the MDM are

$$\mathcal{F}_{a,k} = \sum_{nm \text{ modes}} F_{a,k}, \qquad \mathcal{F}_{c,k} = \sum_{nm \text{ modes}} F_{c,k}. \tag{33}$$

7. Vase form MDM with 12 radial arms: experiment and results

A stainless steel MDM with 12 arms ($K = 12$) was designed and built in quenched Fe87 Cr13 alloy [1] (Fig. 8). Its optical clear aperture is $2a = 160$ mm. Table 1 displays the geometrical parameters of this MDM and the associated intensities of forces $F_{a,k}$ and $F_{c,k}$ applied at $r = a$ and $r = c$ to generate deflections of 10μm peak-to-valley for some Clebsch–Seidel modes. A diagram showing the distribution of Clebsch–Seidel modes of the optical triangular matrix and some He–Ne interferograms obtained with this MDM are displayed by Fig. 9.

Table 1. Distribution of axial forces $F_{a,k}$ and $F_{c,k}$ of a twelve-arm plane MDM ($K = 12$). Quenched Fe87 Cr13 stainless steel, $E = 20510^9$ Pa, $\nu = 0.305$, designed with $t_1 = 8$ mm, $\gamma = (t_1/t_2)^3 = 1/27$, $a = 100$ mm, $b/a = 1.24$ and $c/a = 1.6$. The PtV amplitude of each Clebsch–Seidel mode is $w = 0.1$ mm, i.e., $A_{20} = w/a^2$, $A_{40} = w/a^4$, $A_{31} = w/2a^3$, $A_{22} = A_{20}/2$, $A_{42} = A_{40}/2$ and $A_{33} = A_{31}$

Angle	Arm	Cv 1		Sphe 3*		Coma 3		Astm 3		Astm 5		Tri 5	
	nb.	($n = 2$, $m = 0$)		($n = 4$, $m = 0$)		($n = 3$, $m = 1$)		($n = 2$, $m = 2$)		($n = 4$, $m = 2$)		($n = 3$, $m = 3$)	
θ	k	$F_{a,k}$	$F_{c,k}$	$F_{a,k}$	$F_{c,k}$	$F_{a,k}$	$F_{c,k}$	$F_{a,k}$	$F_{c,k}$	$F_{a,k}$	$F_{c,k}$	$F_{a,k}$	$F_{c,k}$
0	1	−113.3	113.3	−464.0	302.4	−84.0	71.6	154.0	−17.0	168.2	29.9	792	37.3
$\pi/6$	2	−113.3	113.3	−464.0	302.4	−72.7	62.0	77.0	−8.5	84.1	14.9	0	0
$\pi/3$	3	−113.3	113.3	−464.0	302.4	−42.0	35.8	−77.0	8.5	−84.1	−14.9	−792	−37.3
$\pi/2$	4	−113.3	113.3	−464.0	302.4	0.0	0.0	−154.0	17.0	−168.2	−29.9	0	0
$2\pi/3$	5	−113.3	113.3	−464.0	302.4	42.0	−35.8	−77.0	8.5	−84.1	−14.9	792	37.3
$5\pi/6$	6	−113.3	113.3	−464.0	302.4	72.7	−62.0	77.0	−8.5	84.1	14.9	0	0
π	7	−113.3	113.3	−464.0	302.4	84.0	−71.6	154.0	−17.0	168.2	29.9	−792	−37.3
$7\pi/6$	8	−113.3	113.3	−464.0	302.4	72.7	−62.0	77.0	−8.5	84.1	14.9	0	0
$4\pi/3$	9	−113.3	113.3	−464.0	302.4	42.0	−35.8	−77.0	8.5	−84.1	−14.9	792	37.3
$3\pi/2$	10	−113.3	113.3	−464.0	302.4	0.0	0.0	−154.0	17.0	−168.2	−29.9	0	0
$5\pi/3$	11	−113.3	113.3	−464.0	302.4	−42.0	35.8	−77.0	8.5	−84.1	−14.9	−792	−37.3
$11\pi/6$	12	−113.3	113.3	−464.0	302.4	−72.7	62.0	77.0	−8.5	84.1	14.9	0	0

* The uniform load to generate the Sphe 3 mode is $q = 64D_1A_{40} = 0.06172$ MPa.

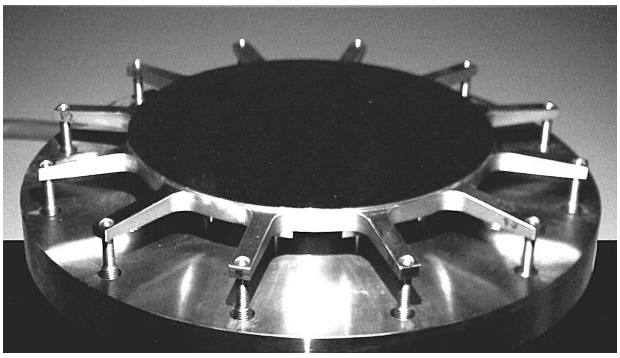

Fig. 8. View of the twelve-arm vase form and plane MDM. Geometrical parameters are $a = 80$ mm, $b/a = 1.25$, $c/a = 1.8125$, $t_1 = 4$ mm, $t_2/t_1 = 1/\gamma^{1/3} = 3$. Elasticity constants of quenched stainless steel Fe87 Cr13 are $E = 2.05{\cdot}10^4$ daN$\cdot$ mm^{-2} and $\nu = 0.305$. Deformation modes are generated by rotation of differential screws at $r = a$ and $r = c$. Air pressure or depressure can be applied onto the rear side of clear aperture $r \leqslant a$ for generating the Sphe 3 mode

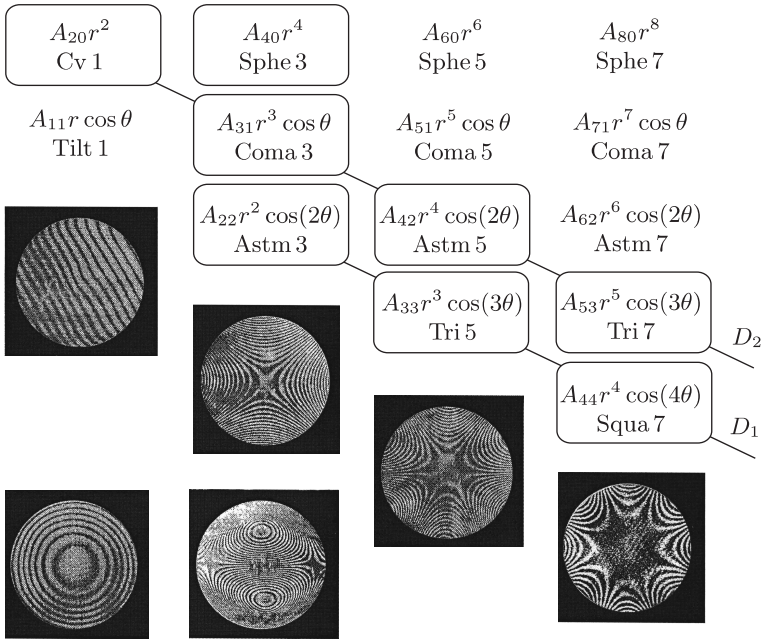

Fig. 9. Upper: Distribution of Clebsch–Seidel modes into the optical triangular matrix (piston z_{00} not shown). When $q = 0$, we obtain $m = n$ modes and $m = n - 2$ modes (D_1 and D_2 diagonal lines). When $q = \text{const}$, we obtain $m = 0$, $n = 4$ mode (upper and second from left).
Lower: He–Ne laser interferograms obtained with the 12-arm vase MDM displayed by Fig. 8.
Upper diagonal boxes: Tilt 1 mode; Astm 3, Tri 5 and Squa 7 modes of D_1 line; lower boxes: Cv 1 and Coma 3 modes of D_2 line

8. Vase form: solutions to generate Astm 3 mode with four forces only

The 3rd-order astigmatism aberration, Astm 3, is caused by the reflection of a non-focused beam on a spherical mirror when the principal ray of the incident beam is not reflected perpendicularly to mirror surface but makes a deviation angle with respect to this incident ray. As a characterization, the reflected beam shows two different curvatures in orthogonal directions.

The correction of Astm 3 can be achieved by use of a deformed plane mirror or a deformed spherical mirror which shape is a *hyperbolic-paraboloid* or a *toroid*, respectively.

Vase form configurations using four forces without arms instead of eight forces with $K = 4$ arms (called degenerated configurations) are presented hereafter for correcting the Astm 3 mode. These configurations bring interesting solutions for practical applications. These solutions, where all $F_{c,k} = 0$, use a vase form and only four forces applied at the rear side of the outer ring.

8.1. Analysis and theoretical results: degenerated configurations

• *Forces $F_{a,k}$ applied to the inner edge of the ring.* Eliminating $F_{a,k}$ in equations (32), we deduce $F_{c,k}$. After nulling these forces, we obtain for the quadrant centered at $\theta = 0$, i.e., $k = 1$,

$$(b-a)\int_{-\pi/4}^{\pi/4} V_r(b,\theta)\,d\theta + \int_{-\pi/4}^{\pi/4} M_r(b,\theta)\,d\theta = 0. \tag{34}$$

Since V_r and M_r have the same modulation in $\cos(2\theta)$, this condition leads, for $\theta = 0$, to

$$(b-a)V_r(b,0) + M_r(b,0) = 0. \tag{35}$$

After substitution of B_{22}, C_{22}, D_{22} and E_{22} coefficients expressed by equation set (31_4), the net shearing force and radial bending moment at $r = b$ are, respectively,

$$V_r(b,0) = -2(1-\nu)D_2A_{22}\left(1-\frac{a}{b}\right)\left[2+\frac{1}{2}(1-\gamma)(1-\nu)\left(1-\frac{a^4}{b^4}\right) - (1-\gamma)(3-\nu)\frac{b^2}{a^2}\right], \tag{36_1}$$

$$M_r(b,0) = 2(1-\nu)D_2A_{22}\left[1-(1-\gamma)\frac{b^2}{a^2}+\frac{1}{4}(1-\gamma)(1-\nu)\left(1-\frac{a^4}{b^4}\right)\right]. \tag{36_2}$$

The substitution in equation (35) leads to the condition

$$1-\frac{a}{b}-\frac{\frac{1}{1-\gamma}-\frac{b^2}{a^2}+\frac{1}{4}(1-\nu)\left(1-\frac{a^4}{b^4}\right)}{\frac{2}{1-\gamma}-(3-\nu)\frac{b^2}{a^2}+\frac{1}{2}(1-\nu)\left(1-\frac{a^4}{b^4}\right)} = 0, \tag{37}$$

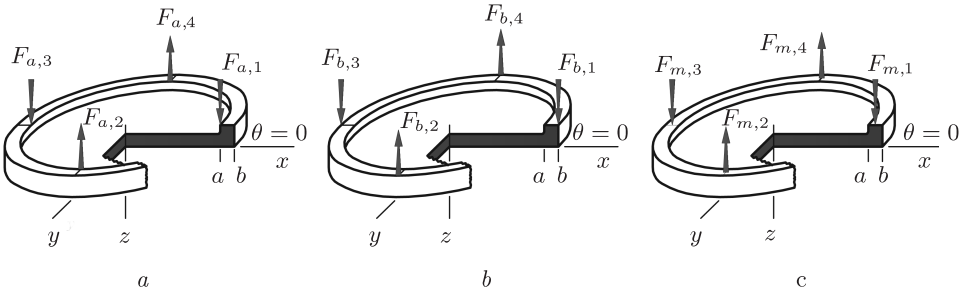

a *b* c

Fig. 10. Vase form configurations generating Astm 3 (primary astigmatism mode) $z_{22} = A_{22}r^2\cos(2\theta)$ with only four forces: *a* – forces $F_{a,k}$ applied to the ring inner edge at $r = a$; *b* – forces $F_{b,k}$ applied to the ring outer edge at $r = b$; *c* – force $F_{m,k}$ applied to the mid-circle of the ring rear surface. This latter configuration is most convenient for practical applications

where $\gamma = D_1/D_2 = (t_1/t_2)^{1/3} < 1$. Although the b/a ratio must be close to unity for practicable reasons, solutions t_2/t_1 can be found for $a < b < 1.15a$ (Fig. 10; Table 2).

Table 2. Solutions for vase form mirror geometries generating the Astm 3 mode z_{22} with only four forces $F_{a,k}$, i.e., $\forall F_{c,k} = 0$, applied at the inner edge $r = a$ of the ring. The ratios b/a and t_2/t_1 are given with respect to Poisson's coefficient ν

b/a	t_2/t_1		
	$\nu = 0.15$	$\nu = 0.20$	$\nu = 0.30$
1.050	2.21	2.22	2.23
1.075	1.96	1.96	1.97
1.100	1.80	1.80	1.81
1.125	1.69	1.69	1.70
1.150	1.60	1.61	1.62

• *Forces $F_{b,k}$ applied to the outer edge of the ring.* Assuming that the forces applied to each end of radial arms at $r = b$ and $r = c$ are denoted $F_{b,k}$ and $F_{c,k}$, respectively, the equations for statics equilibrium read, for $k = 1, 2, 3, 4$,

$$F_{b,k} + F_{c,k} = b\int_{\pi(2k-3)/4}^{\pi(2k-1)/4} V_r(b,\theta)\,d\theta, \tag{38_1}$$

$$(c-b)F_{c,k} = b\int_{\pi(2k-3)/4}^{\pi(2k-1)/4} M_r(b,\theta)\,d\theta. \tag{38_2}$$

Researching a condition for nulling $F_{c,k}$, from (3_1) and (14_3) we have for the outer ring

$$M_r = D_2\left[\frac{\partial^2 z}{\partial r^2} + \nu\left(\frac{1}{r}\frac{\partial z}{\partial r} + \frac{1}{r^2}\frac{\partial^2 z}{\partial\theta^2}\right)\right], \tag{39}$$

$$z = R_{22}\cos(2\theta) = (B_{22}r^2 + C_{22}r^{-2} + D_{22}r^4 + E_{22})\cos(2\theta), \tag{40}$$

where the rigidity D_2 of the outer ring is a constant. This leads to

$$M_r = 2D_2\big[(1-\nu)B_{22} + 3(1-\nu)C_{22}r^{-4} + 6D_{22}r^2\big]\cos(2\theta). \tag{41}$$

The integration on θ from $-\pi/4$ to $\pi/4$ of equation (38_2) is not necessary since one searches to null M_r for nulling $F_{c,k}$. Then, using the analytical value of coefficients B_{22}, C_{22}, D_{22} and E_{22} in (31_4), a necessary condition is given by $M_r(r=b,\theta=0)=0$. After substitution and simplification, we obtain the condition

$$\frac{4}{1-\gamma} + 1 - \nu - (1-\nu)\frac{a^4}{b^4} - 4\frac{b^2}{a^2} = 0, \tag{42}$$

where $\gamma = D_1/D_2 = (t_1/t_2)^{1/3} < 1$.

This equation allows solutions t_2/t_1 for b/a-ratios such as $1 < b/a < 1.15$ (Fig. 10, b; Table 3).

Table 3. Solutions for vase form mirror geometries generating the Astm 3 mode z_{22} with only four forces $F_{b,k}$, i.e., $\forall\, F_{c,k} = 0$, applied at the outer edge $r = b$ of the ring. The ratios b/a and t_2/t_1 are given with respect to Poisson's coefficient ν

b/a	t_2/t_1		
	$\nu = 0.15$	$\nu = 0.20$	$\nu = 0.30$
1.050	2.54	2.52	2.47
1.075	2.21	2.19	2.15
1.100	2.00	1.98	1.95
1.125	1.85	1.84	1.82
1.150	1.74	1.73	1.71

• *Forces $F_{m,k}$ applied to the mid-circle of the ring rear area.* For practical reasons it has been found convenient to achieve the astigmatism deformation Astm 3 of a vase form mirror with four orthogonal forces $F_{m,k}$ applied at the mid-circle $r = \frac{1}{2}(a+b)$ of the rear side of the outer ring (Fig. 10, c). The corresponding vase form geometries with $F_{c,k} = 0$ can be deduced by adopting the mean values t_2/t_1 of previous Tables 2, 3 (Table 4).

Table 4. Solutions for vase form mirror geometries generating the Astm 3 mode $z_{22} = A_{22}r^2\cos(2\theta)$ with only four forces $F_{m,k}$ applied at the mid-circle $r = \frac{1}{2}(a+b)$ of the rear surface of the ring. The ratios b/a and t_2/t_1 are given with respect to Poisson's coefficient ν

b/a	t_2/t_1		
	$\nu = 0.15$	$\nu = 0.20$	$\nu = 0.30$
1.050	2.38	2.37	2.35
1.075	2.08	2.07	2.06
1.100	1.90	1.89	1.88
1.125	1.77	1.76	1.76
1.150	1.67	1.67	1.66

8.2. Boundary conditions for practical applications

The above solutions for generating the Astm 3 mode provide a pure and accurate parabolic flexure in radial directions, however obtaining an accurate $\cos(2\theta)$ modulation along the perimeter surface requires use of appropriate boundary conditions. Since each of four $F_{m,k}$ forces are discrete, as results from integrations of a continuous force distribution $f\cos(2\theta)\,d\theta$ which should be applied all along the perimeter, it is preferable not to apply the four forces directly to the outer ring but to adopt one of the following alternative designs.

• *Outer ring with variation of the axial thickness.* The rear side of the ring departs from a flat surface and shows four wedged shapes where each forces $F_{m,k}$ are applied. The variation of the axial thickness t_2 along the ring distributes a smooth and accurate flexure in $\cos(2\theta)$ with only four forces applied at the wedges. The axial thickness $t_2(\theta)$ in a quadrant, designed and optimized by Hugot et al. [13], [14], is

$$t_2(\theta) = \lambda t_1 \left[\frac{1/2 - 2\theta/\pi}{\cos(2\theta)}\right]^{1/3}, \qquad 0 \leqslant \theta \leqslant \frac{\pi}{2}, \tag{43}$$

which satisfies $t_2(\theta) = t_2(\pi/2 - \theta)$ and leads to $t_2(0)/t_2(\pi/4) = \sqrt[3]{\pi/2} = 1.162\ldots$, and where λ is a constant depending on b/a, ν and E. In fact, the four wedges are not made angularly sharp but show a square flat area to allow sealing a removable metal part used for the force applications with springs (Fig. 11). This alternative vase form has been designed and built for three spherical concave mirrors in Zerodur ($\nu = 0.24$) and it is bring to various toroid shapes by stress figuring. These off-axis mirrors belong to the main optical train of SPHERE, the new planet finder instrument of ESO's VLT.

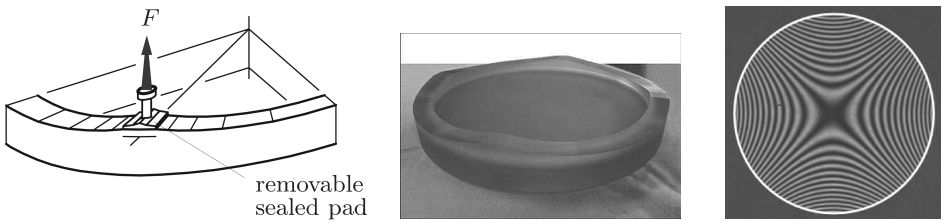

a *b* *c*

Fig. 11. *a* – alternative design for obtaining a pure $\cos(2\theta)$ modulation of the flexure with four discrete axial forces $F_{m,k}$ applied to a four-wedged outer ring of thickness $t_2(\theta)$; *b* – view of one of three Zerodur toroid mirrors of the SPHERE planet finder optical train installed at ESO's VLT; *c* – He–Ne interferogram of the Astm 3 saddle-like asphericsation after stress polishing and elastic relaxation

• *Outer ring with forces acting on angular bridges.* In this alternative design one still has a ring of constant thickness t_2, but instead of directly applying the external force $F_{m,k}$ in a direction where the angular modulations are at maximum amplitude, one

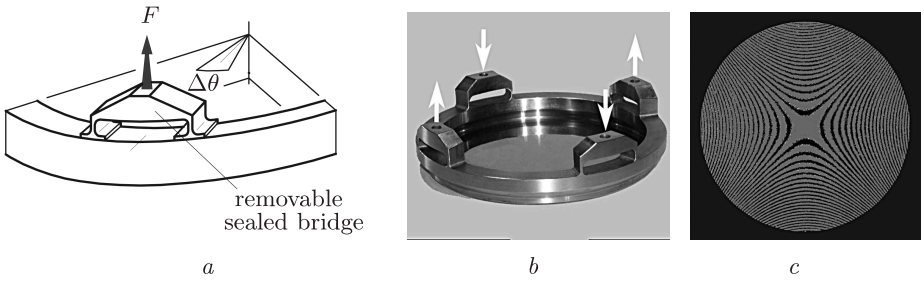

Fig. 12. *a* – alternative design for obtaining a pure $\cos(2\theta)$ modulated flexure by keeping the ring axial thickness $t_2 = \text{const}$, the four forces $F_{m,k}$ are subdivided into eight forces via orthogonal bridges with $\Delta\theta = 22.5^\circ$ angular arch separation; *b* – view of the one-piece stainless steel matrix for making concave toroid gratings, via replicas, for the single surface spectrographs CDS and UVCS of the SOHO Mission; *c* – He–Ne fringes of the Astm 3 saddle-like aspherisation

subdivides each forces into two equal force components via bridges linked to the ring. Each of four forces acts at the center of a bridge. The two arch feet are linked to the ring by tangentially thin ends that are equivalent to articulations. These bridges can be made of metal and removable for glass mirror substrates. A smooth and accurate $\cos(2\theta)$ modulation of the flexure is achieved when the angular separation of the two arch ends is $\Delta\theta = \pi/16 = 22.5^\circ$.

Deformable active matrices with four bridges (Fig. 12) were first designed and built for making (via replications process) the toroid gratings of *single surface* spectrographs CDS and UVCS of the SOHO Mission (ESA/NASA) for solar studies at Lagrange point L_1. In this case, the thickness t_1 was not a constant but of the cycloid-like form $(1 - r^2/a^2)^{1/3}$ simply supported by thin collar to the outer ring [1].

For applications, a detailed geometry of each above *vase form* alternatives can be optimized with finite element analysis. Besides, we make a design under the maximum admissible stress σ_{ult} of the material substrate, so it is useful to determine the bending force intensities. Starting from equation (38_1), using equation set (31_4), and assuming that b and a are about similar, i.e., $F_{m,k} \simeq F_{b,k}$, we obtain as a first approximation for $k = 1$

$$F_{m,1} \simeq F_{b,1} = -(1-\nu)(1-\gamma)\left[\frac{4}{1-\gamma} + 1 - \nu + (1-\nu)\frac{a^4}{b^4} - 2(3-\nu)\frac{b^2}{a^2}\right] D_2 A_{22}. \quad (44)$$

From condition given by equation (42), for the four forces we have

$$F_{m,k} = -(-1)^k 2(1-\nu)^2(1-\gamma)\left(\frac{b^2}{a^2} - \frac{a^4}{b^4}\right) D_2 A_{22}, \qquad k = 1, 2, 3, 4. \quad (45)$$

This set of forces is by itself in static equilibrium, i.e., self-reacting.

9. Conclusions

Deformable vase form substrates can provide a highly accurate flexure for correcting the primary astigmatism aberration Astm 3 within diffraction limited criteria. Two alternative boundary configurations applied to this design allow use of four self-reacting forces only if they are located far from the optical surface in agreement with Saint-Venant's principle.

The substrate material can be either a vitro-ceram glass such as Zerodur or a metal alloy with linear stress–strain relationship as chromium stainless steel in a quenched state. Vase form designs will find many applications for large telescope mirror segments used off-axis and also in astronomical optics as off-axis mirrors of unobstructed planet finder instruments and for obtaining saddle-shaped concave gratings used in spectrographs [1], [15].

More generally, other Clebsch–Seidel modes $r^n \cos(m\theta)$, such as those with $m = n$, can be also accurately generated from vase form geometries and by use of four forces only.

The author is grateful to Patrice Joulié for the execution of drawings in the figures.

References

1. Lemaitre G. R. *Astronomical optics and elasticity theory – active optics methods.* Springer, Berlin, 2010.
2. Lemaitre G. R. *Compensation des aberrations par élasticité.* Nouv. Rev. Opt., **5-6** (1974), 361–366.
3. Kirchhoff G. R. *Uber das gleichewicht und die bewegung iener elastischen scheibe.* J. Crelle, **40** (1850), 51–88.
4. Kirchhoff G. R. *Vorlesungen über mathematische physik: Mechanik.* Teubner, Leipzig, 1877.
5. Lemaitre G. R. *Active optics: Vase or meniscus multimode mirrors and degenerated monomode configurations.* Meccanica, **40**:3 (2005), 233–249.
6. Lubliner J., Nelson J. E. *Stress mirror polishing.* Appl. Opt., **19**:14 (1980), 2332–2340.
7. Timoshenko S.P., Woinowsky-Krieger S. *Theory of Plates and Shells.* McGraw-Hill, New York, 1959.
8. Reissner E. *Stresses and small displacements of shallow spherical shells.* I. II. J. Math. Phys., **25** (1946), 80–85; 279–300.
9. Landau L.D., Lifshitz E. M. *Theory of elasticiy.* Pergamon Press, Oxford, 1970; transl. from Rus.: *Théorie de l'Elasticité*, Mir, M., 1967.
10. Clebsch A. R. F. *Theorie der elasticität fester Körper.* B. G. Teubner, Stuttgart, 1862; French transl.: de Saint-Venant B. A. J.-C., Flamant A. *Théorie de l'Elasticité des Corps Solides*, Dunod, Paris, 1883.
11. de Saint-Venant B. A. J.-C. *Mémoire sur la Torsion des Prismes.* Mémoire des Savants Étrangers Acad. Sci. Paris, **14** (1855), 233–560.
12. Germain P., Mulller P. *Introduction à la Mécanique des Milieux Continus.* Masson, Paris, 1995.

13. Hugot E., Ferrari M., El Hadi K., Vola P., Gimenaz J.-L., Lemaitre G. R., Rabou P., Dohlen K., Beuzit J.-L., Hubin N. *Active Optics: stress polishing of toric mirrors for the* Vlt Sphere *adaptive optics system.* Appl. Opt., **48** (2009), 2932–2941.

14. Hugot E., Ferrari M., El Hadi K., Costille A., Dohlen K., Pujet P., Beuzit J.-L. *Active optics methods for exoplanet direct imaging. Stress polishing of supersmooth aspherics for VLT-SPHERE planet finder.* Astron. Astrophys., **538** (2012), A139, 4 pp.

15. Lemaitre G. R. *Active optics with a minimum number of actuators.* Adv. Opt. Tech., **3**:3 (2014), 223–249.

Gérard R. Lemaitre
Laboratoire d'Astrophysique de Marseille,
Marseille, France, EU
E-mail: gerard.lemaitre@lam.fr

Received 05.01.2015